Supporting Information

The in vitro selectivity and in vivo specificity of the nickel metallochaperone, SlyD

H. Kaluarachchi, Judith F. Siebel, Supipi Kaluarachchi-Duffy, Sandra Krecisz, D. E. K. Sutherland, M. J. Stillman and D. B. Zamble

METHODS

PAR competition experiments. A competition reaction was set up as noted in equation (A) by adding increasing amounts of apo SlyD to separate aliquots of 400 μM PAR containing 8 μM Zn(II) in 20 mM HEPES pH 7.5, 100 mM NaCl.

$$Zn(PAR)_2 + SlyD \rightleftarrows Zn\text{-}SlyD + 2PAR \qquad K_{ex1} \qquad (A)$$

Samples were equilibrated overnight at 4 ^{o}C and subsequently analyzed by electronic absorption spectroscopy at 500 nm. Titrations of 400 μM PAR with Zn(II) under identical conditions were used to calculate the amount of [Zn-PAR_2] formed in the competition (A). The pH of the solution affects the formation constant of the Zn-PAR_2 complex as well as the molar absorption coefficient (ε) of this complex, so the metal-binding affinity of PAR under these particular buffer conditions was calibrated using EGTA as described in detail by Zimmerman et al (*1*). Briefly, increasing amounts of EGTA were titrated into 400 μM PAR containing 8 μM Zn(II) to achieve a competition as noted in (B).

$$Zn(PAR)_2 + EGTA \rightleftarrows Zn\text{-}EGTA + 2PAR \qquad K_{ex2} \qquad (B)$$

An average K_D of SlyD for zinc was then obtained from equation (C) (derived from combining reactions A and B) where the known formation constant for Zn-EGTA corrected for pH (K_a = $10^{9.39}$) was used (*2*).

$$K_{D\ (Zn\text{-}SlyD)} = K_{D\ (Zn\text{-}EGTA)} \times (K_{ex2}/K_{ex1}) \qquad (C)$$

Bcs competition experiments. All experiments were set up and equilibrated in an anaerobic glovebox using buffers that were degassed with Argon for several hours. Apo protein samples were titrated into a solution of $[Cu(Bcs)_2]^{3-}$ of defined molar ratio L:Cu(I) ≥ 2.5, where the

chelator concentration was kept high enough to ensure negligible contribution from the 1:1 Cu:L complex. In these mixtures, the ligand and copper concentrations were held constant while varying the concentration of the protein. Transfer of Cu(I) from the chelator to protein or vice versa can be detected by the change in absorbance at 483 nm for Bcs (*1*). By systematically varying the concentration of the chelators and the protein, conditions that favoured competition were achieved. From the resulting spectra the K_D of SlyD for Cu(I) was determined.

Co(II) affinity using Fura2. A stock solution of 35 μM Fura-2 (Invitrogen) containing 8-12 μM Co(II) was obtained by incubating the metal with the chelator for 30 min at room temperature. The free dye concentration was determined by using electronic absorption spectroscopy and the reported extinction coefficient of 28000 M^{-1} cm^{-1} at 363 nm (*3*). To achieve competitive conditions as noted in reaction (D), increasing amounts of apo SlyD were added to separate aliquots of this cobalt-Fura2 solution and allowed to equilibrate overnight at 4 ^{o}C in an anaerobic glovebox.

$$[\text{Co(II)-Fura2}] + \text{SlyD} \rightleftarrows \text{Co-SlyD} + \text{Fura2} \qquad K_{ex3} \tag{D}$$

$$K_{D\,(\text{Co-SlyD})} = (K_{ex3})^{-1}\, K_{D\,(\text{Co-Fura2})} \tag{E}$$

The resulting solutions were analyzed using electronic absorption spectroscopy at 368 nm, which indicates the amount of chelator bound to cobalt. An extinction coefficient of 24000 M^{-1} cm^{-1} at 368 nm was measured by titration of Fura2 with the $CoSO_4$ alone under identical conditions and used for calculating the concentration of Co(II)-Fura-2 present at each titration point. An average K_D of Co-SlyD was then calculated using data from several replicates via equation (E). A K_D of 8.64 x 10^{-9} M reported for the [Co(II)-Fura2] complex at pH 7.0 (*4*), was used in these calculations because the affinity of this chelator to metal is constant near neutral pH (*5*).

TABLES

Table S1. Summary of metal concentrations used for metal toxicity studies.

Growth Condition	Metal tested	[Metal(II))] μM
LB media Aerobic	Co(II)	100, 200, 500, 1000, 10000*
	Ni(II)	100, 200, 500, 1000, 10000*
	Cu(II)	100, 200, 500, 1000*
	Zn(II)	100, 200, 500, 1000, 10000*
Minimal media Aerobic	Co(II)	10, 100*
	Ni(II)	10, 30*, 100*
	Cu(II)	10, 100, 250*†
	Zn(II)	10, 150, 300, 400, 700*†

*No growth was detected for the wildtype and *ΔslyD* strains indicating lethal metal concentrations. †A slight precipitate was detected upon addition of the metal to minimal media.

Table S2. Primers used for qRT-PCR.

Primer Name	Sequences (5' → 3')
znuA forward	ACATGCATCTTTGGCTTTCC
znuA reverse	TGCCTCAAAATCCTTCAGGT
zntA forward	AGAAAGCCCCTCAATTTGCT
zntA reverse	CCGGAGACGTTTTCAGAGAG
copA forward	CAAGCCAGAAATCGGTCAGC
copA reverse	CAAAGAAATACCAGATTGCCGC
cusF forward	ATGAAACCATGAGCGAAGCACA
cusF reverse	CGGATCGTGATGGATGGTGAT
nikA forward	CAGTGCTCGATAACCGTCAA
nikA reverse	GCGCTTTTCAGGGTAATTTG
rcnA forward	GAACCAGGGCACTCAAAAAC
rcnA reverse	TGCGGTATGCGAAATAGTTG
holB forward	GCTTAGGTGGTGCGAAAGTC
holB reverse	GTTTCTGCTGGTGGCTCTTC

Table S3. Metal stoichiometry of WT SlyD[†].

Metal	*Ni (II)*	*Mn (II)*	*Co(II)*
Mn(II)		0.2 ± 0.1	
Co(II)			3.9 ± 0.1
Ni(II)	4.2 ± 0.3		
Ni(II) & Mn(II)	4.0 ± 0.2	n/d*	
Ni(II) & Co(II)	4.4 ± 0.1		n/d*

[†]Stoichiometries were determined by using equilibrium dialysis in which 40 μM apo SlyD samples were dialyzed against an equal volume of 320 μM metal overnight at 4 ^{o}C in an anaerobic glovebox. *n/d, a protein-metal complex for the particular metal was not detected.

FIGURES

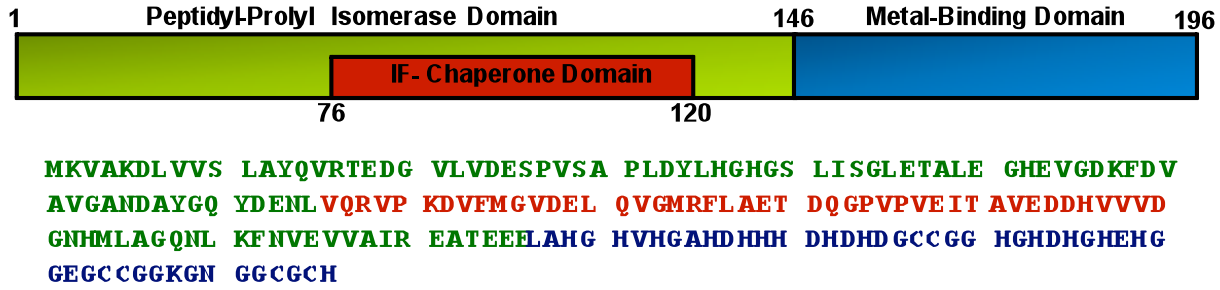

Figure S1. Domain organization and amino acid sequence of *E. coli* SlyD. The N-terminus of SlyD encompass the FKBP-type peptidyl-prolyl isomerase (PPIase) domain and the chaperone domain termed insertion in the flap (IF domain). The C-terminus corresponds to the metal-binding domain of SlyD that contains several number of potential metal-binding residues such as Cys, His, Asp and Glu (*6*). The amino acid sequence has been colour coded to match the domain accordingly.

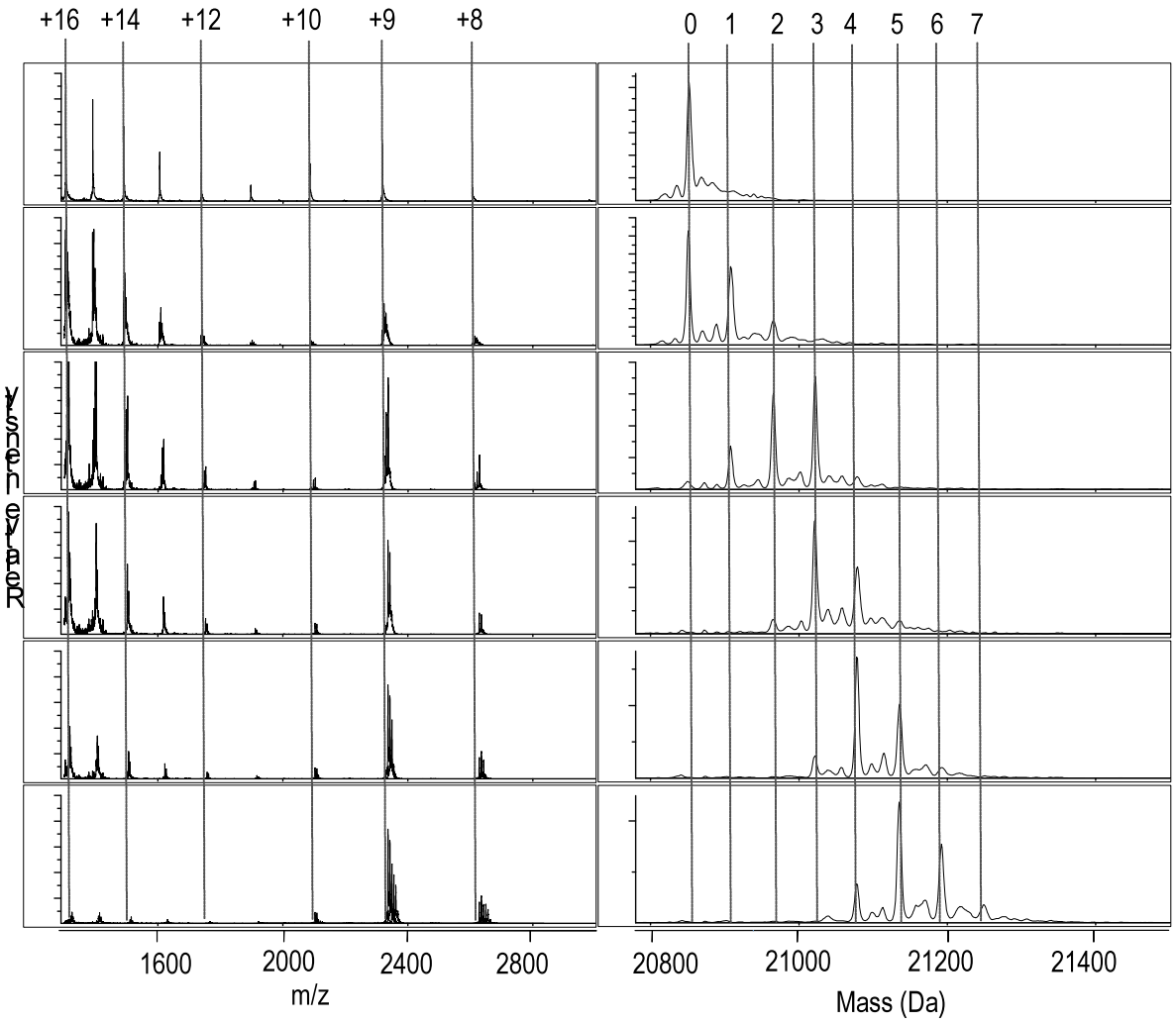

Figure S2. Re-evaluating Ni(II) binding to SlyD by ESI-MS. The m/z spectra (left panels) and the reconstructed spectra (right panels) are from a Ni(II) titration analyzed on the mass spectrometer equipped with the HSID interface. The addition of increasing concentrations of nickel acetate to the apo protein (10 μM) results in simultaneous metal loading to multiple metal sites, which is indicative of a non-cooperative Ni(II)-binding mechanism. The molar equivalents of nickel added relative to protein concentration from top to bottom is: 0, 0.6, 2.1, 3.5, 4.2, 6 The numbers heading the dotted-line represent the number of nickel ions bound to the protein (right panels) and the charge state of SlyD (left panels).

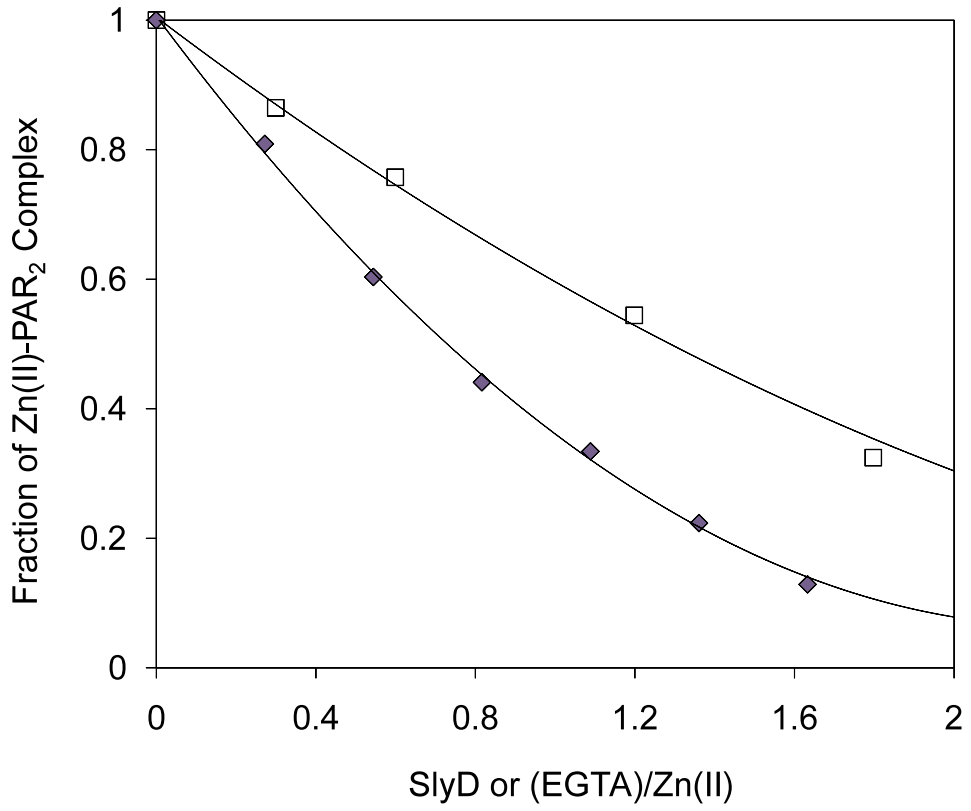

Figure S3. Determining the Zn(II) dissociation constant (K_D) of SlyD using PAR. The change in the amount of Zn(II)-PAR_2 complex was monitored at 500 nm upon addition of increasing amounts of apo SlyD (filled diamonds) or EGTA (unfilled squares). Titrations were conducted in 20 mM HEPES pH 7.5, 100 mM NaCl with a $[PAR]_{Total}$ = 400 μM and $[Zn(II)]_{Total}$ = 8 μM. SlyD is more effective than EGTA at pH 7.5 at competing with PAR for zinc, indicating $K_{D(Zn\text{-}SlyD)} < K_{D\ (Zn\text{-}EGTA)}$ of $10^{-9.3}$ M.

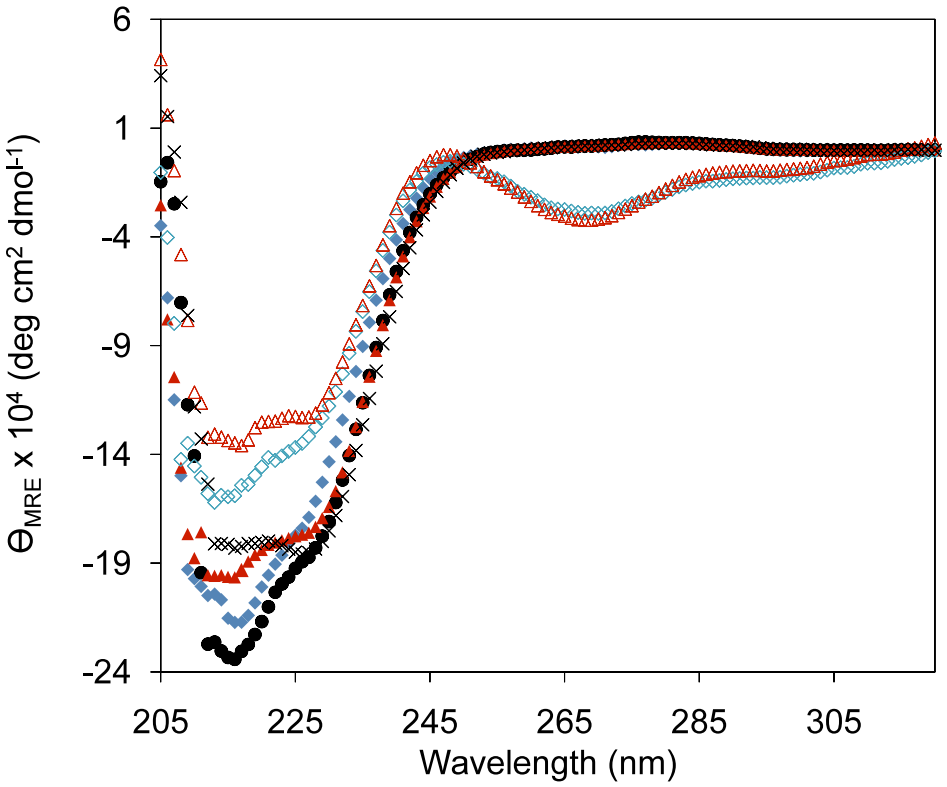

Figure S4. Comparison of Ni(II)- vs. Zn(II)-induced secondary structure changes in SlyD. A decrease in the mean residue ellipticity is detected in the far-UV region as compared to the apo protein (60 μM) spectrum (filled circles) following incubation with metal. The spectra for the metal-loaded SlyD are: 2 equiv. Zn(II) (filled diamonds), 2 equiv. Ni(II) (unfilled diamonds), 4 equiv. Zn(II) (filled triangles), 4 equiv. Ni(II) (unfilled triangles) and 8 equiv. Zn(II) (black crosses).

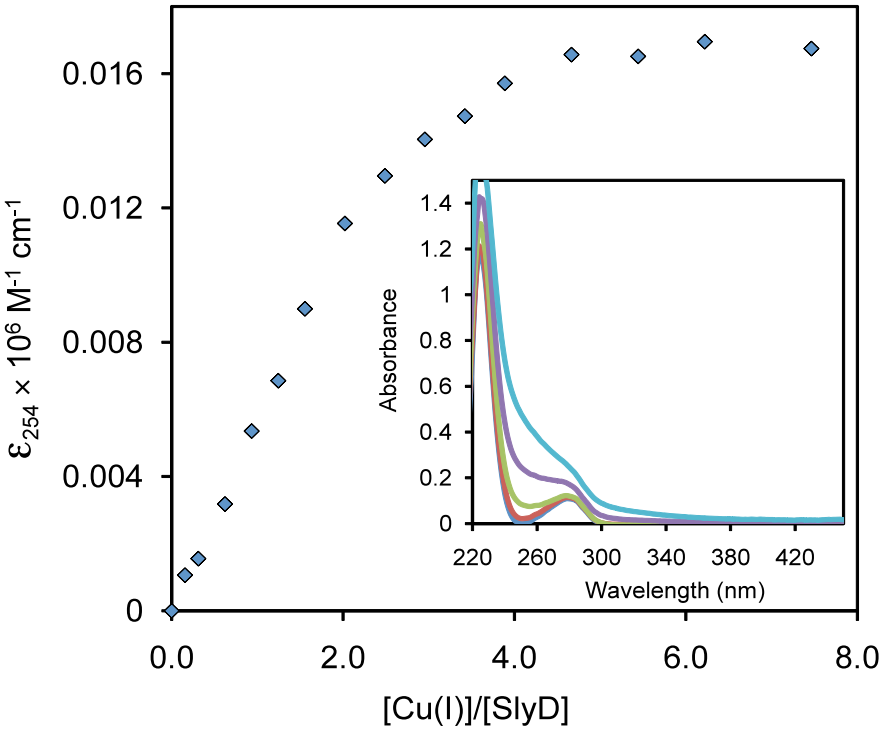

Figure S5. Visualizing Cu(I) binding to SlyD. An anaerobic titration of apo SlyD (25 μM) with increasing Cu(I) results in the appearance of a charge transfer band at ~ 254 nm, indicative of Cu(I) binding to thiolate ligands (inset). A plot of ε_{254} versus equivalents of copper indicates saturation around ~4-5 equivalents of Cu(I) added.

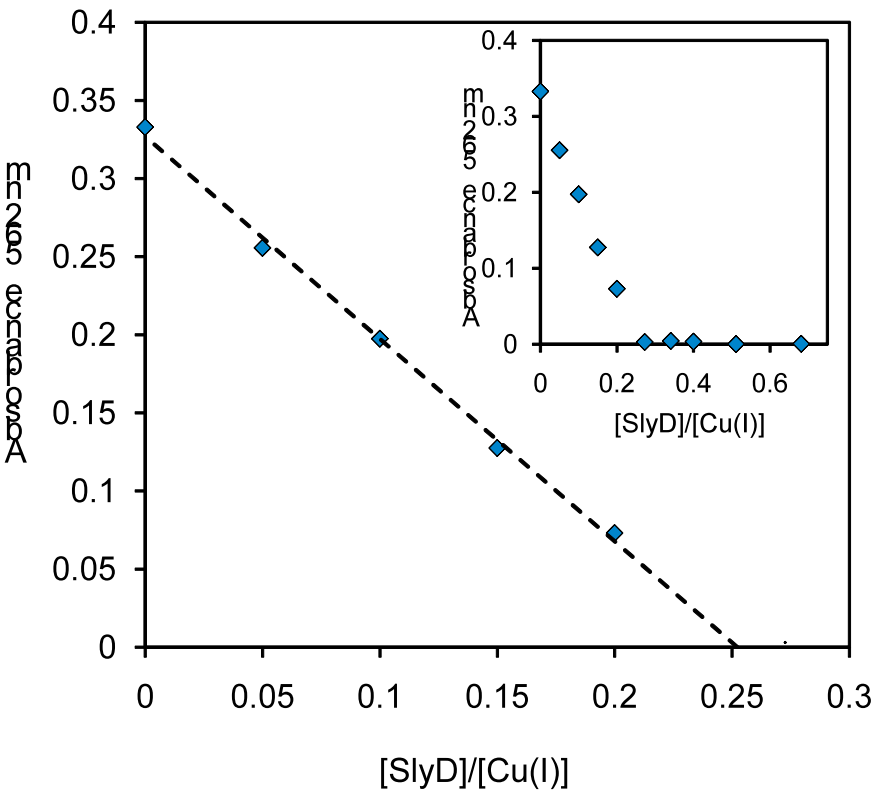

Figure S6. Stoichiometry of SlyD for Cu(I). Titration of apo SlyD into a solution of 100 μM Bca containing 40 μM Cu(I) results in a linear decrease in the absorbance at 562 nm. A linear fit of the data reveals that at 0.25 [SlyD]/[Cu(I)] all the Cu(I) is removed from Bca by the protein, indicating a stoichiometry of 4 Cu(I)/SlyD monomer.

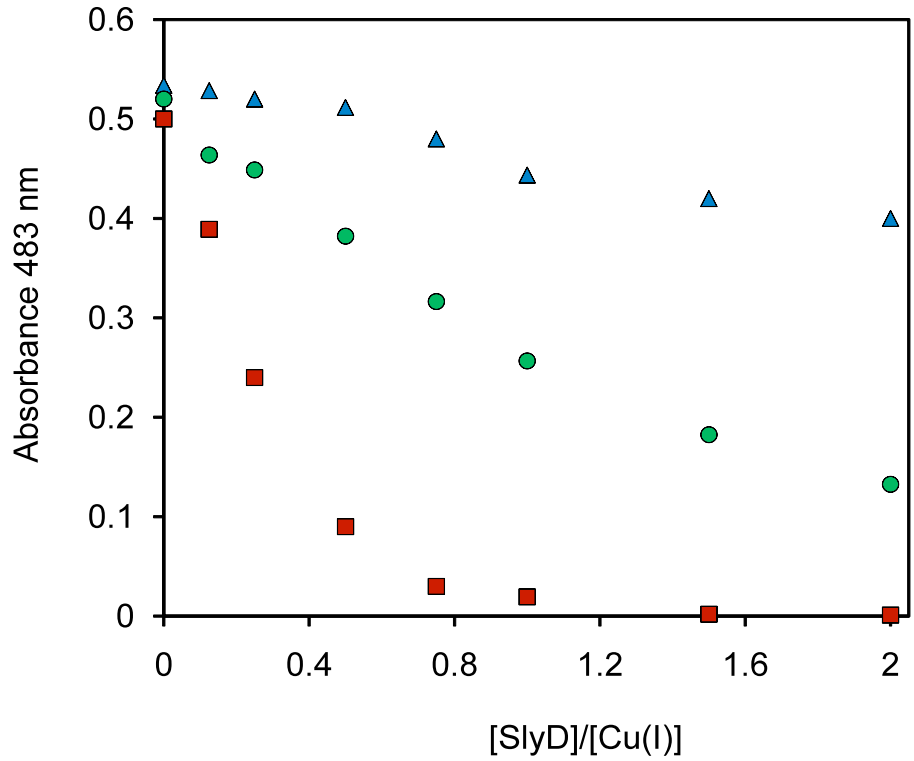

Figure S7. Determining the Cu(I) K_D for SlyD. The change in the absorbance at 483 nm was monitored upon addition of apo SlyD to solutions with a constant Cu(I) concentration of 40 μM and $[Bcs]_{total}$ = 100 μM (squares), 300 μM (circles), or 500 μM (triangles). The non-linear decrease in the absorption with increasing protein concentration is indicative of competitive conditions for Cu(I) binding.

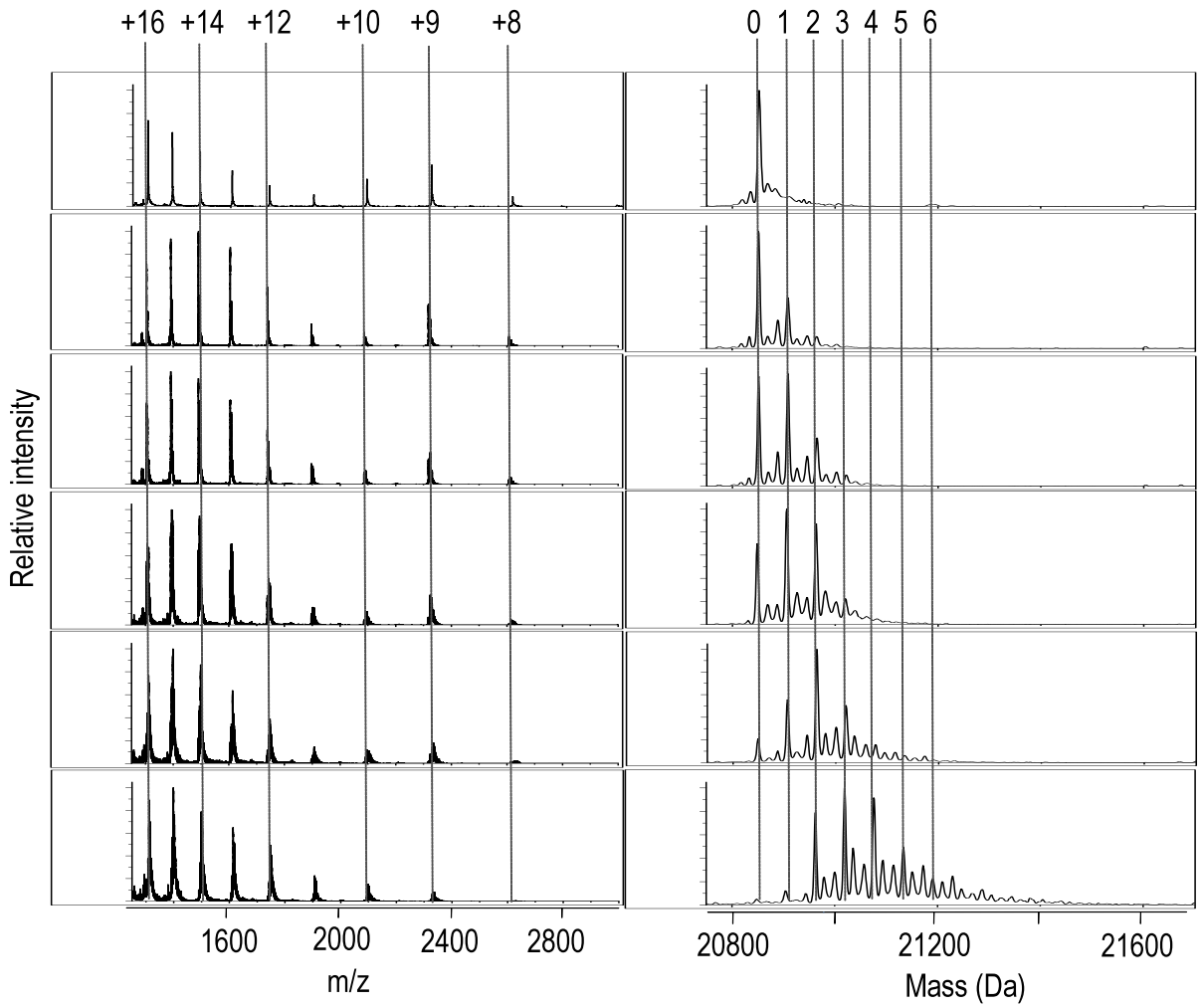

Figure S8. ESI-MS titration of WT SlyD with Co(II) in the presence of 100 μM DTT. The addition of increasing amounts of Co(II) to SlyD (10 μM) leads to concurrent filling of multiple metal sites indicating a non-cooperative metal-binding mechanism. From top to bottom the equivalents of Co(II) added relative to protein concentration are: 0, 1, 2.5, 3.5, 4.4, and 7. The m/z spectra are shown on the left with the respective reconstructed spectra on the right. The numbers heading the dotted-lines indicate the number of Co(II) ions bound to SlyD (right panels) and the charge states of the protein (left panels). The amount of Co(II)-SlyD appears to be less than the total Co(II) added to the solution when DTT is included in the protein buffer, suggesting the reducing agent competes with SlyD for cobalt coordination.

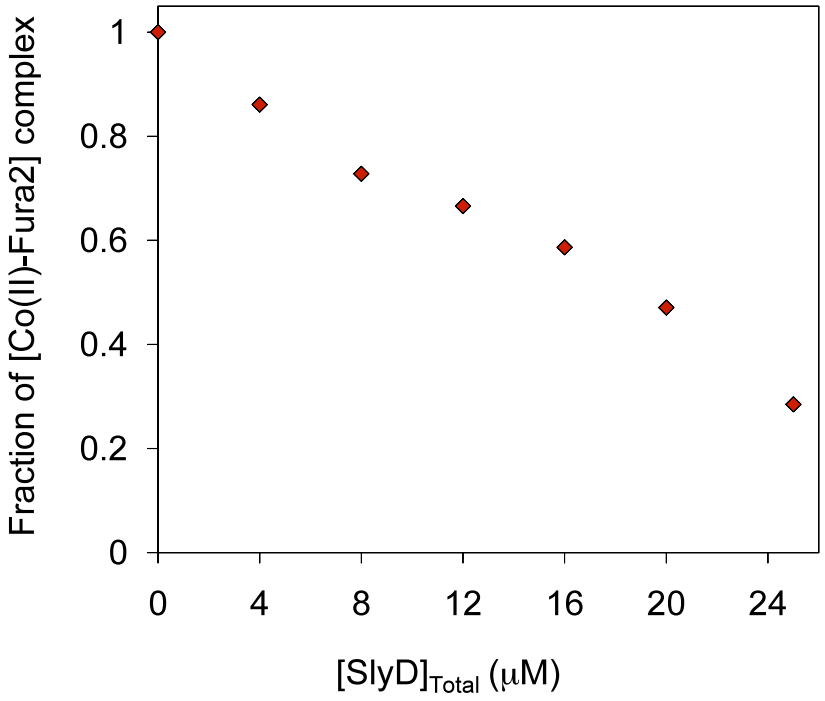

Figure S9. Affinity of SlyD for Co(II) via Fura-2 competition. Titration of apo SlyD into a solution of Co(II) (10 μM) and Fura-2 (35 μM) leads to a decrease in the amount of [Co(II)-Fura2]$^{2-}$ in solution that is detected by the absorbance at 368 nm. From competition titrations such as that shown an apparent $K_{D\ (Co(II)\text{-}SlyD)}$ of $4 \pm 1 \times 10^{-9}$ M was obtained.

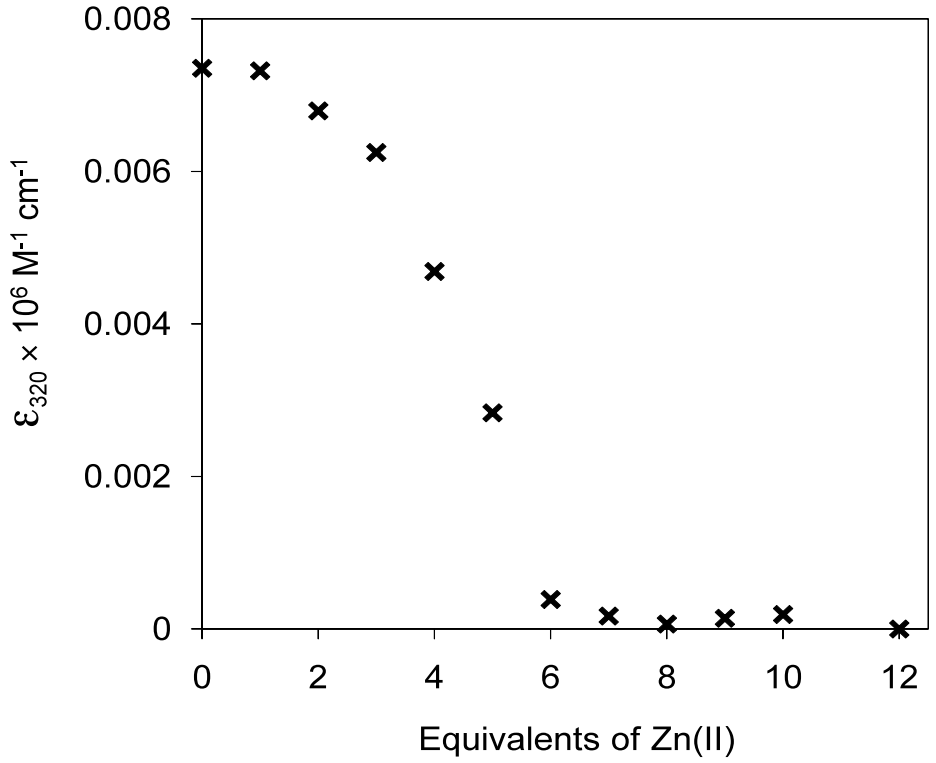

Figure S10. Zn(II) can replace Co(II) bound to SlyD. The addition of increasing amounts of Zn(II) to a SlyD sample (25 μM) saturated with Co(II) (200 μM) leads to a decrease in the signal at 320 nm, indicating that Zn(II) can effectively replace all of the Co(II) from metal sites composed of thiolate ligands.

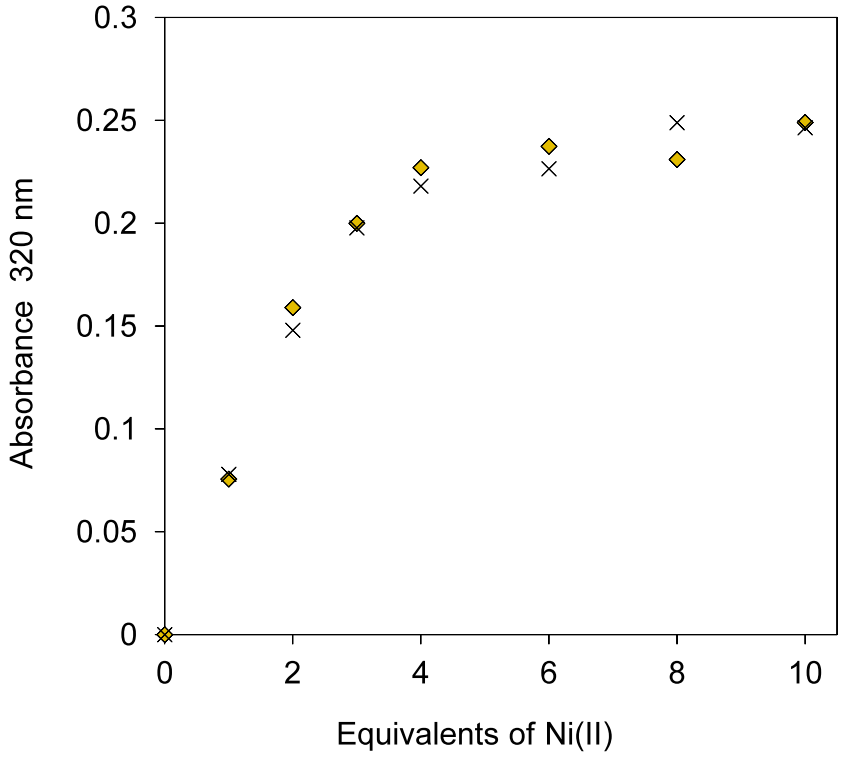

Figure S11. Selectivity of SlyD for Ni(II) vs. Fe(II). The change in absorbance at 315 nm upon titration of apo SlyD (20 μM) with Ni(II) (crosses) is shown. A similar titration curve is obtained when adding Ni(II) to a SlyD sample (20 μM) pre-incubated with 200 μM Fe(II) (diamonds), indicating that Ni(II) coordination to the protein is unperturbed in the presence of excess Fe(II).

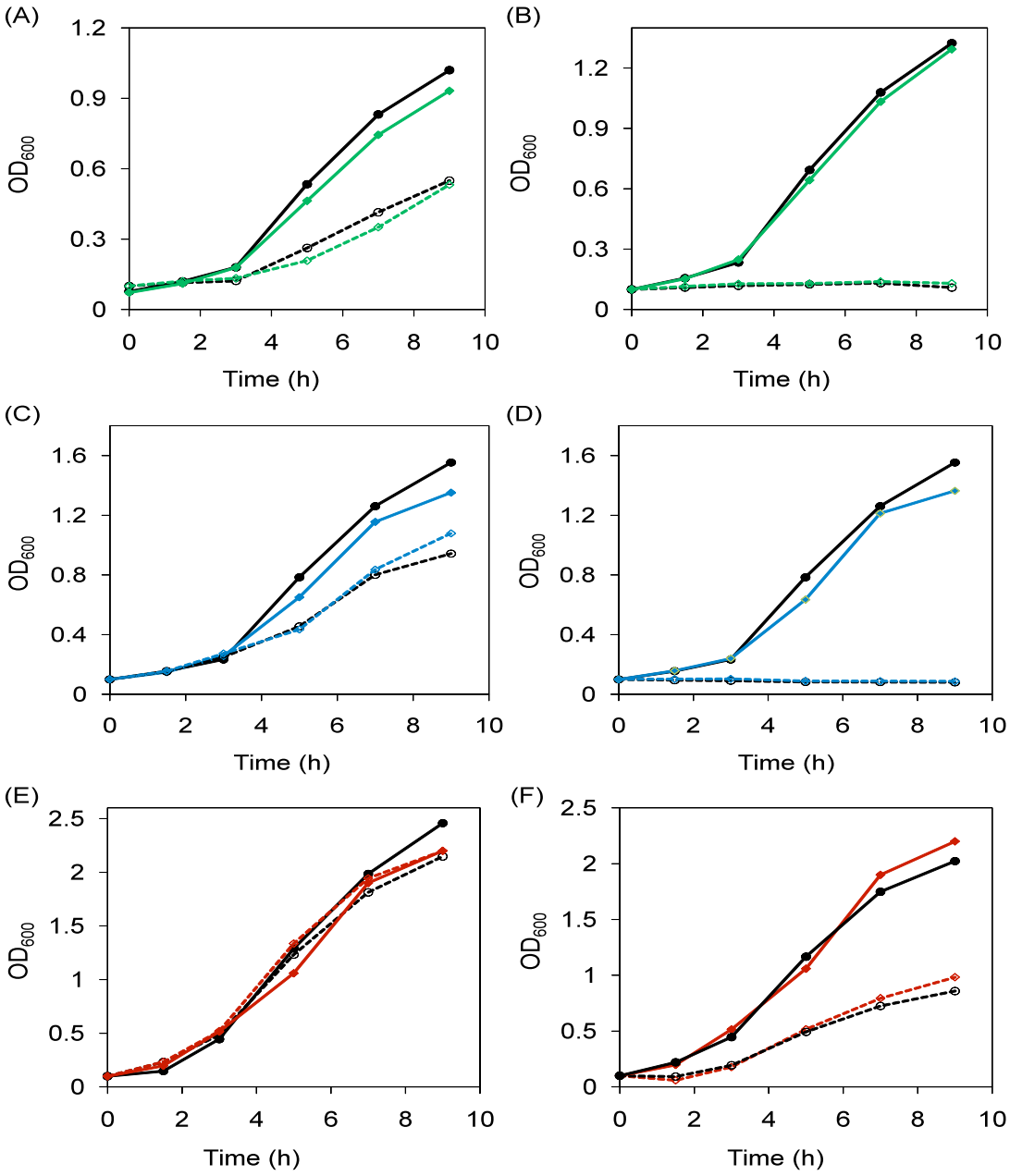

Figure S12. Sensitivity of *E. coli* to transition metals. Representative data set for the growth rates of wildtype and *ΔslyD* strains of *E. coli* upon addition of various metal concentrations as detected via OD_{600}. These experiments were conducted in minimal media supplemented with: (A) 10 μM Ni(II), (B) 30μM Ni(II), (C) 50 μM Cu(II), (D) 250 μM Cu(II), (E) 150 μM Zn(II), (F) 500 μM Zn(II). The black lines correspond to the wildtype strain and the coloured lines indicate the growth detected for the *ΔslyD* strain. The solid lines and the dashed lines represent growth detected in untreated and treated cultures, respectively.

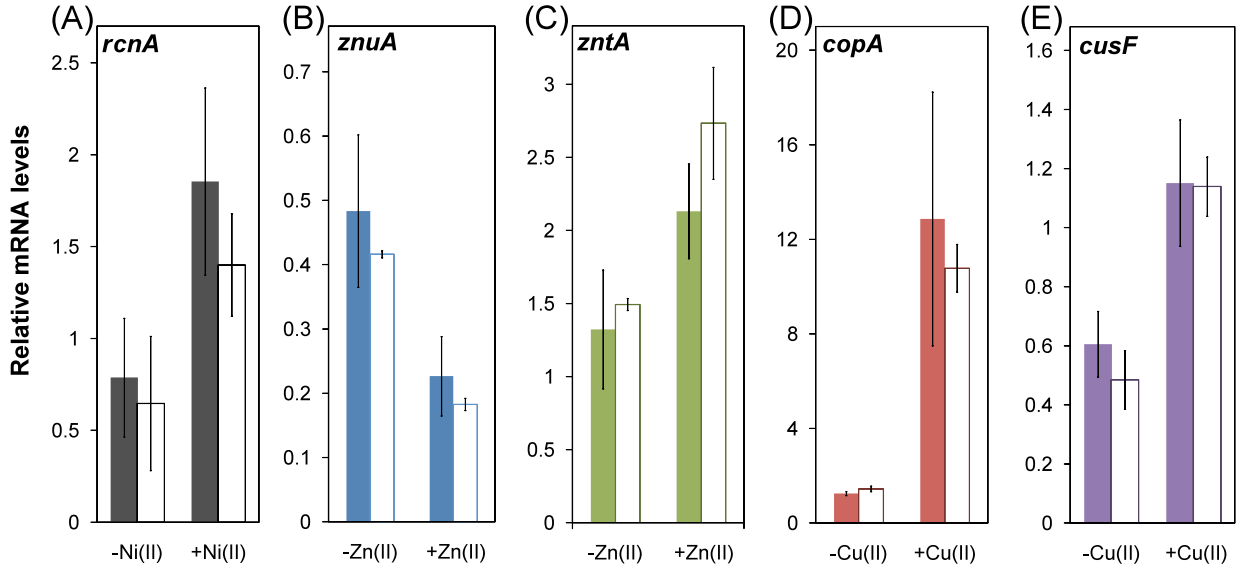

Figure S13. Expression profiles of zinc, copper and nickel transporters from aerobic growths. Relative mRNA levels detected upon addition of 10 μM Ni(II) (Panel A), 400 μM Zn(II) (Panels B-C) and 150 μM Cu(II) (Panels D-E). The bars denoted –Zn(II), -Cu(II) or -Ni(II) correspond to bacteria cultured in minimal media without added metal. The mRNA detected for each transcript in the wildtype and *ΔslyD* strains are shown in solid and clear bars, respectively. The reported relative mRNA levels were normalized with respect to *holB*, which encodes a DNA gyrase. A p-value > 0.05 was calculated for the transcript levels of the wildtype and *ΔslyD* strains, indicating no significant difference between the two strains.

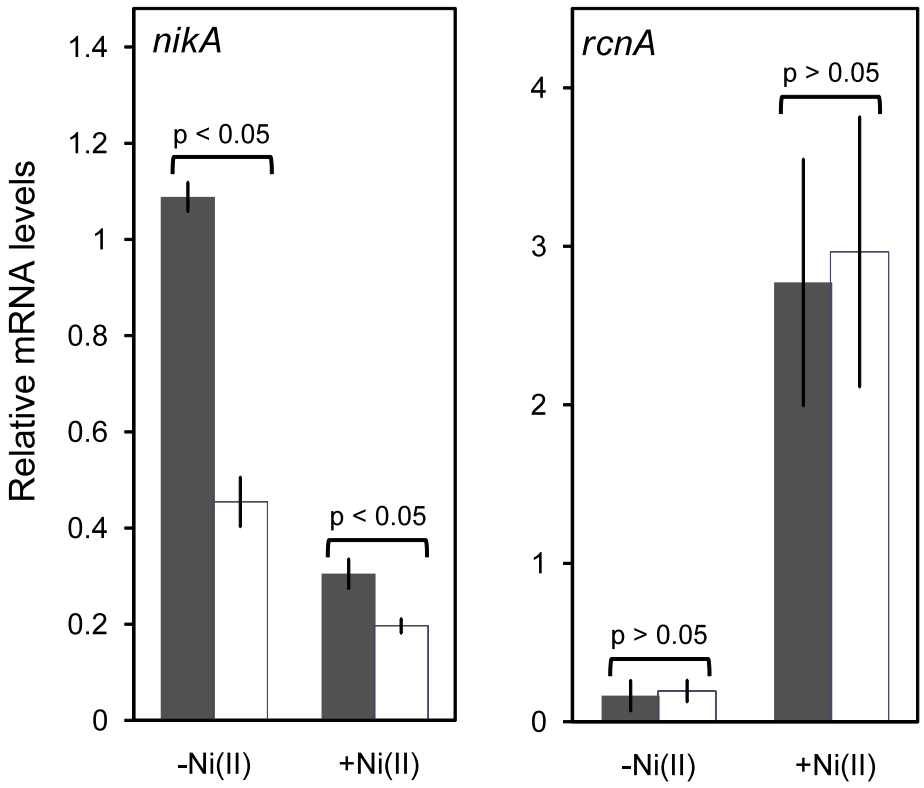

Figure S14. Expression the Ni(II) transporters in the presence of excess Zn(II). Relative change in mRNA levels of *nikA* and *rcnA* detected upon addition of 10 μM Ni(II) and 400 μM Zn(II). Bacteria were grown in media optimized for hydrogenase expression under anaerobic conditions. The bars denoted –Ni(II) correspond to bacteria cultured in media without added metal. The mRNA detected for each transcript in the wildtype and Δ*slyD* strain under identical growth conditions are shown in solid and clear bars, respectively. The reported relative mRNA levels were normalized with respect to *holB*, which encodes a DNA gyrase. The p-values (based on student t-test) < 0.05 indicate the data sets are significantly different whereas p-values > 0.05 are considered to be not significantly different.

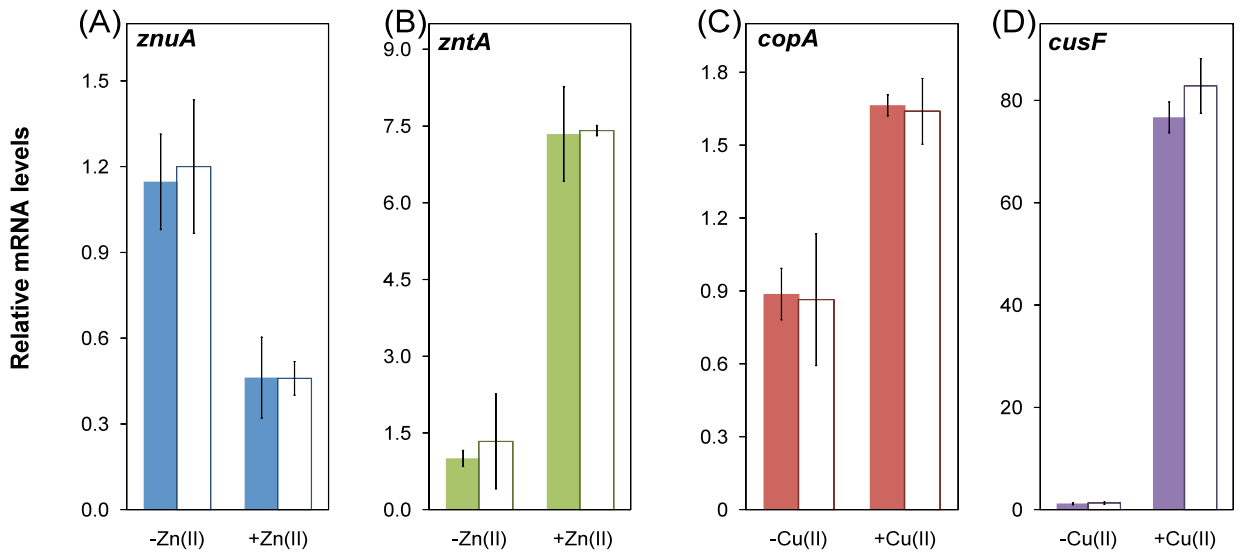

Figure S15. Expression profiles of zinc and copper under anaerobic growth conditions. Relative mRNA levels detected upon addition of 400 μM Zn(II) (Panels A-B) or 150 μM Cu(II) (Panels C-D). The bars denoted –Zn(II) or -Cu(II) correspond to bacteria cultured in minimal media without added metal. The mRNA detected for each transcript in the wildtype and *ΔslyD* strains under identical growth conditions are shown in solid and clear bars respectively. The reported relative mRNA levels were normalized with respect to *holB*, which encodes a DNA gyrase. A p-value > 0.05 was calculated for the wildtype and *ΔslyD* strains for all transcripts, indicating no significant difference between the two strains.

REFERENCES

1. Zimmermann, M., Clarke, O., Gulbis, J. M., Keizer, D. W., Jarvis, R. S., Cobbett, C. S., Hinds, M. G., Xiao, Z. G., and Wedd, A. G. (2009) Metal Binding Affinities of *Arabidopsis* Zinc and Copper Transporters: Selectivities Match the Relative, but Not the Absolute, Affinities of their Amino-Terminal Domains, *Biochemistry 48*, 11640-11654.
2. Fahrni, C. J., and O'Halloran, T. V. (1999) Aqueous coordination chemistry of quinoline-based fluorescence probes for the biological chemistry of zinc, *J. Am. Chem. Soc. 121*, 11448-11458.
3. Golynskiy, M. V., Gunderson, W. A., Hendrich, M. P., and Cohen, S. M. (2006) Metal binding studies and EPR spectroscopy of the manganese transport regulator MntR, *Biochemistry 45*, 15359-15372.
4. Kwan, C. Y., and Putney, J. W. (1990) Uptake and Intracellular Sequestration of Divalent-Cations in Resting and Methacholine-Stimulated Mouse Lacrimal Acinar-Cells - Dissociation by Sr-2+ and Ba-2+ of Agonist-Stimulated Divalent-Cation Entry from the Refilling of the Agonist-Sensitive Intracellular Pool, *J. Biol. Chem. 265*, 678-684.
5. Grynkiewicz, G., Poenie, M., and Tsien, R. Y. (1985) A new generation of Ca^{2+} indicators with greatly improved fluorescence properties, *J. Biol. Chem. 260*, 3440-3450.
6. Wulfing, C., Lombardero, J., and Pluckthun, A. (1994) An *Escherichia coli* protein consisting of a domain homologous to FK506-binding proteins (FKBP) and a new metal binding motif, *J. Biol. Chem. 269*, 2895-2901.